CRITICAL ANALYSIS OF CAPACITOR-COMMUTATED CONVERTERS (CCC)

José Alberto Fernandes Ferreira Jr. Ricardo Paulino Marques Walter Kaiser
Escola Politécnica da Universidade de São Paulo – Depto. PEA ,
Av. Prof. Luciano Gualberto Trav.3 nº158 CEP:05508-900 São Paulo, SP - Brasil
jaffjunior@yahoo.com rpm@lac.usp.br kaiser@lac.usp.br

***Abstract* – Capacitors in series with the AC branches in line-commutated converters improve DC voltage regulation and extend operation beyond the normally attainable control angles. This paper presents the operating characteristic of capacitor–commutated converters, including valve voltage stress and attainable control range for particular capacitor values, for a wide DC load current range. Also mathematical formulations of DC voltage versus current characteristic and commutation angles versus current are presented for thyristor rectifiers.**

***Keywords* – Capacitor-commutated converter, HVDC, Rectifier**

I. INTRODUCTION

The capacitor-commutated converter (CCC) is a conventional line commutated three-phase bridge converter with capacitors in series with the AC phase connections. The capacitors reduce the reactive power requirements and provide an additional voltage contribution to the valves allowing commutation in firing angle regions normally unattainable in conventional converters. Potential applications in HVDC transmission have been reported [1,4,5,6] and functional products using this technology are already available [5,6]. This converter has also potential application in other special high power applications such as in electrolysis rectifiers.

The basic equations describing steady-state operation of the CCC were first proposed in [1]. The aim of this paper is to establish a thorough understanding of the capacitive commutation technique and also provide a critical analysis of the converter parameters at load current variations.

II. VOLTAGE REGULATION IN BRIDGE RECTIFIER CONVERTERS

The general principles employed in the analysis of the bridge rectifier converter under steady state conditions, fully covered in the literature [2,3], have been directed at situations where AC branches are purely inductive and assume continuous and perfectly smoothed DC current as indicated in Fig. 1.

The odd (1,3,5) and even (2,4,6) valves are associated with the positive G_+ and negative G_- half-bridges respectively. Transition of the current from one valve to the other cannot take place instantaneously because of reactances in the AC branches and the transition period is known as commutation period or overlapping angle μ.

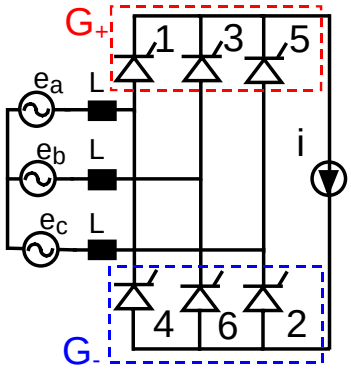

Fig. 1. Three-phase bridge rectifier with inductive commutation

The rectifier's DC voltage versus current curve encompasses three operation modes (see Fig. 2). Within the normal load range, the rectifier operates in MODE 1, with independent commutation in both half bridges. Also only one valve of each half bridge carries current between successive overlap periods. When DC current increases, the rectifier operates in MODE 2, with independent commutation in both half bridges. However, in this mode the converter operates continuously in the commutation process. At higher DC currents, the rectifier operates in MODE 3 with three or four valves conducting simultaneously and commutations in both half-bridge circuits interfering with each other.

Instead of assuming an approximate relation between alternating and direct currents, a common scaling factor is used in order to obtain consistent equations irrespective of the side of the converter taken as reference. For convenience, DC open circuit voltage U_o and peak value of phase-to-phase short circuit current I_{sc} are proposed [2] as voltage and current base values in the following analysis.

$$V_{BASE} = U_O = \frac{3 \cdot \sqrt{3} \cdot E_m}{\pi}, \quad (1)$$

$$I_{BASE} = I_{SC} = \frac{\sqrt{3} \cdot E_m}{2 \cdot \omega \cdot L}, \quad (2)$$

where E_m is the phase-to-neutral voltage peak value and L is the commutation inductance.

Figure 2 shows the normalized DC voltage versus current curve and Fig. 3 presents the behavior of overlap angle μ as a function of the normalized DC current of the three phase bridge from no-load to short-circuit for various firing angle values [3].

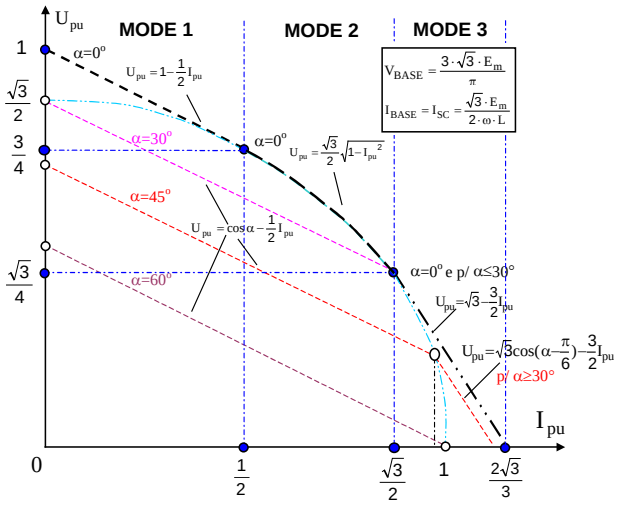

Fig. 2. Three-phase bridge rectifier - DC voltage versus current.

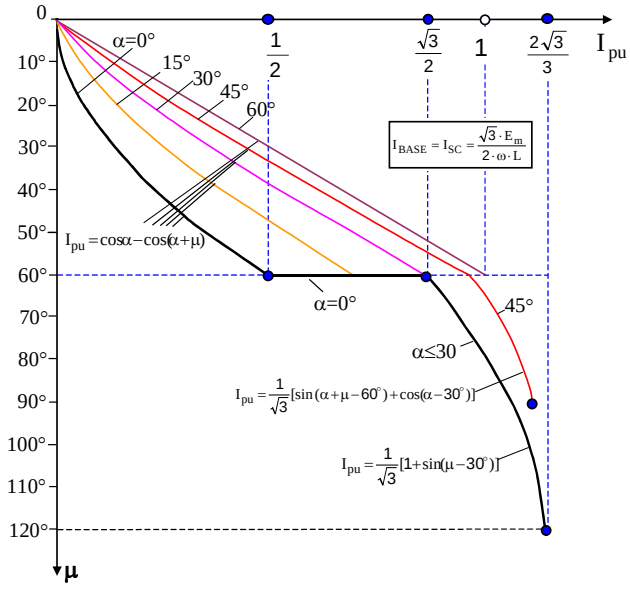

Fig. 3. Three-phase bridge rectifier – Overlap angle μ versus current.

III. CCC ELEMENTARY MODE OF OPERATION

Figure 4 shows the three-phase full-wave bridge converter configuration with added series capacitors. Neglecting line inductances, the capacitor voltages are trapezoidal and in steady state their mean voltages are null.

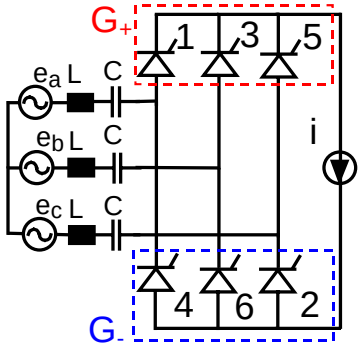

Fig. 4. Three-phase rectifier with capacitive commutation

The peak value of the capacitor voltages is independent of the commutation overlap and given by:

$$V_{C\max} = \frac{\pi}{3} \cdot \frac{I}{\omega \cdot C}, \qquad (3)$$

where, C is the commutation capacitance, I is the DC load current, V_{Cmax} is the maximum capacitor voltage and ω is the line frequency.

Figure 5 shows the composition of the phase voltages and capacitor voltages that produces the shifted commutation voltages U_{RECT} at the rectifier output. The capacitor allows the rectifier to operate with negative firing angles α. The extent to which the firing angle can be advanced beyond the normal region (inductive commutation) depends on the phase shift with respect to original AC supply waveform.

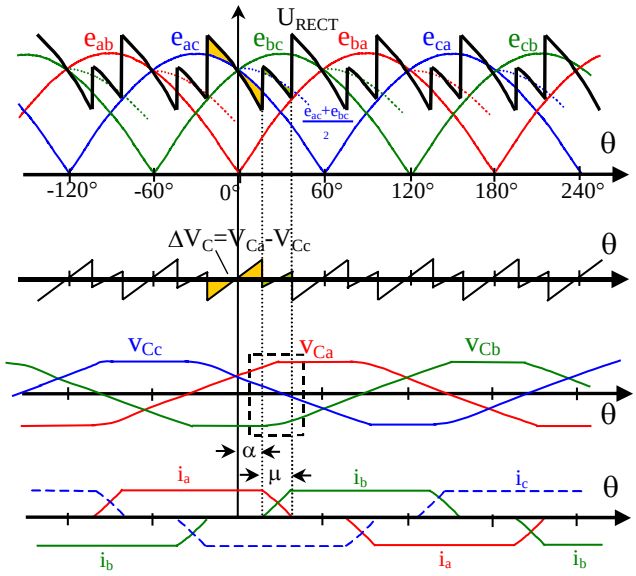

Fig. 5. DC rectifier voltage, capacitor voltages and currents.

A more realistic system description should take in to account the inductive line impedances and therefore additional capacitor voltage changes ΔV_1 and ΔV_2 appear during commutation for outgoing and incoming phases, as shown in the detail of Fig.6.

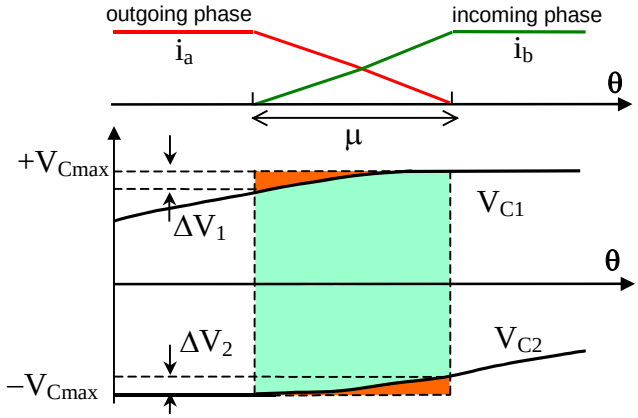

Fig. 6. Detail of additional capacitor voltage changes ΔV1 and ΔV2 due to the inductor during commutation.

IV. ANALYTICAL FORMULATION OF THE CCC COMMUTATION PROCESS

The following assumptions for modeling apply: i) AC voltage is stiff and may be represented by an ideal sinusoidal source in series with a lossless inductance, ii) DC current is ripple-free and constant, iii) valves are ideal with zero on-resistance and infinite off-resistance; changes between these two states are instantaneous and iv) valves are fired at intervals of one sixth of a cycle (60°). The converter will be analyzed only within the normal load range where the commutations in both half-bridge circuits proceed independently. For convenience, DC open circuit voltage U_o and peak value of phase-to-phase short circuit current I_{sc} as in (2) are proposed as voltage and current base values in the following analysis.

A. Computation of commutation current and ovelap angle.

Figure 7 presents the frequency domain equivalent circuit of the commutation from valve 1 to valve 3. The voltage source LI denotes the initial condition of full direct current in the outgoing phase.

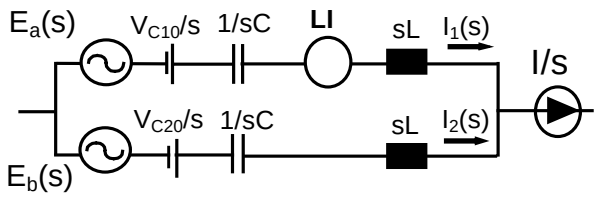

Fig. 7. Equivalent circuit of the CCC during commutation from valve 1 to valve 3.

At the beginning of the commutation, the capacitors in the incoming and outgoing phases are charged to:

$$V_{C2_0} = -\frac{\pi}{3}\cdot\frac{I}{\omega\cdot C}, \tag{4}$$

$$V_{C1_0} = \frac{\pi}{3}\cdot\frac{I}{\omega\cdot C} - \Delta V_1, \tag{5}$$

where ΔV_1 is the change of the capacitor voltage during commutation in the outgoing phase. Correspondingly, the change of the capacitor voltage in the incoming phase will be denoted ΔV_2. The sum of these terms is given by;

$$\Delta V_1 + \Delta V_2 = \frac{\mu\cdot I}{\omega\cdot C}, \tag{6}$$

where μ is the commutation angle (see Fig. 4).

The instantaneous line-to-neutral $e(\theta)$ and corresponding line-to-line $v(\theta)$ voltages of the ac sources are given by:

$$\begin{aligned} e_a &= E_m\cdot\cos(\theta+\tfrac{\pi}{3}) & v_{ac} &= \sqrt{3}\cdot E_m\cdot\cos(\theta+\tfrac{\pi}{6}) \\ e_b &= E_m\cdot\cos(\theta-\tfrac{\pi}{3}) & v_{ba} &= \sqrt{3}\cdot E_m\cdot\cos(\theta-\tfrac{\pi}{2}) \\ e_c &= E_m\cdot\cos(\theta-\pi) & v_{cb} &= \sqrt{3}\cdot E_m\cdot\cos(\theta+\tfrac{5\pi}{6}) \end{aligned} \tag{7}$$

With reference to Fig. 7, substituting the initial conditions given in (4) and (5) and adopting the base values defined in (1) and (2) the normalized Laplace transform of the outgoing phase current is:

$$I_{1_{pu}}(s) = \frac{I_{PU}/2}{s} - \frac{\frac{\cos\alpha}{k^2-1}\cdot s - \frac{\sin\alpha}{k^2-1}\cdot\omega}{s^2+\omega^2} + \frac{-\left(\frac{\cos\alpha}{k^2-1}+\frac{I_{pu}}{2}\right)\cdot s + [\frac{\pi k}{3}\cdot I_{pu} - \frac{3}{\pi\cdot k}\cdot\Delta V_{1_{pu}} + \frac{k}{k^2-1}\cdot\sin\alpha]\cdot\omega_o}{s^2+\omega_o{}^2}, \tag{8}$$

where:

I_{pu} DC current p.u. value;
α firing angle;
$\Delta V_{1_{pu}}$ outgoing capacitor voltage change in p.u.;
ω_o $\frac{1}{\sqrt{L\cdot C}}$;
k $\frac{\omega_o}{\omega}$.

Equation (8) in the time domain is given by

$$\begin{aligned} i_{1_{pu}}(\theta) = I_{pu}\cdot(&\frac{1}{2} - \frac{\pi}{3}\cdot k\cdot\sin(k\theta) + \frac{1}{2}\cdot\cos(k\theta)) + \\ &+ \frac{1}{k^2-1}(-\cos(\theta+\alpha) + \cos\alpha\cdot\cos(k\theta) - k\cdot\sin\alpha\cdot\sin(k\theta)) \cdot \\ &+ \frac{3}{\pi\cdot k}\cdot\Delta V1_{pu}\cdot\sin(k\theta). \end{aligned} \tag{9}$$

At end of commutation the outgoing current vanishes, i.e., $i_1(\mu) = 0$ and therefore

$$\Delta V_{1_{pu}} = [\frac{\cos\frac{\mu}{2}\cdot tg\frac{k\mu}{2} - k\cdot\sin\frac{\mu}{2}}{k^2-1}\cdot\cos(\alpha+\tfrac{\mu}{2}) + \frac{k\cdot\mu}{4}\cdot I_{pu}]\cdot\frac{k\cdot\pi}{3}. \tag{10}$$

Another expression relating I_{pu} with ΔV_{1pu} results from the fact that $\Delta V_1 = \frac{1}{\omega C}\int_0^{\mu} i_1(\theta)d\theta$ and is given by

$$\Delta V_{1_{pu}} = \frac{-k\cdot\sin(\alpha+\mu) + \cos\alpha\cdot\sin k\mu + k\cdot\sin\alpha\cdot\cos k\mu}{(k^2-1)\cdot(\cos(k\mu)+1)}\cdot\frac{k\cdot\pi}{3} + \frac{[k(\frac{1}{2}\mu-\frac{\pi}{3}) + \frac{1}{2}\sin k\mu + \frac{k\cdot\pi}{3}\cos k\mu]}{\cos(k\mu)+1}\cdot\frac{k\cdot\pi}{3}\cdot I_{pu}. \tag{11}$$

From (10) and (11) I_{pu} is given by

$$I_{pu} = 2\cdot\frac{(k\cdot tg\frac{k\mu}{2}\cdot\cos\frac{\mu}{2} - \sin\frac{\mu}{2})}{k(\frac{\mu}{2}-\frac{2\pi}{3})\cdot tg\frac{k\mu}{2}+1}\cdot\frac{\sin(\alpha+\frac{\mu}{2})}{k^2-1}. \tag{12}$$

B. Commutation conditions.

In a three-phase bridge rectifier commutation can only take place when the valves involved are directly polarized. Therefore the following voltage conditions in outgoing and incoming phases have to be met:

$$v_{in} - v_{cap_{in}} > v_{out} - v_{cap_{out}}. \tag{13}$$

The admissible firing angle condition is given by:

$$\sin\alpha \geq -\frac{\pi k^2}{3}\cdot I_{pu} + \frac{3}{\pi}\cdot\Delta V_{1_{pu}}. \tag{14}$$

An expression for the admissible firing angles is obtained from (10) and (12) in (14).

$$\operatorname{tg}\alpha \le \frac{k^2\cdot(\mu-\frac{4\pi}{3})(\cos k\mu-\cos\mu)+k^2\cdot\sin\mu\cdot(1+\cos k\mu)-k\cdot\sin k\mu\cdot(1+\cos\mu)}{k\cdot(\mu-\frac{4\pi}{3})(\sin k\mu-k\cdot\sin\mu)+(2-k^2-k^2\cdot\cos\mu)(1+\cos k\mu)-k\cdot\sin\mu\cdot\sin k\mu} \quad (15)$$

C. Mean DC bridge output voltage.

The normalized mean direct voltage over a complete cycle as a function of control angle α and commutation angle μ is given by

$$U_{pu}=\frac{U}{U_o}=\frac{3}{\pi\cdot U_o}\left[\int_{\alpha}^{\mu+\alpha} v_{rect\ com\ pu}\,d\theta+\int_{\mu+\alpha}^{\frac{\pi}{3}+\alpha} v_{rect\ without\ com\ pu}\,d\theta\right] \quad (16)$$

$$U_{pu}=\frac{3}{\pi}\left[\int_{\alpha}^{\mu+\alpha}\left(\frac{\sqrt{3}\cdot\pi}{6}\cdot\cos(\theta)-I_{pu}\frac{\pi\cdot k^2}{4}\cdot(\theta-\alpha)+\frac{3}{2}\Delta V_{1_{pu}}\right)d\theta+\right.$$

$$\left.+\int_{\mu+\alpha}^{\frac{\pi}{3}+\alpha}\left(\frac{\pi}{3}\cos(\theta-\frac{\pi}{6})-I_{pu}\cdot\frac{\pi\cdot k^2}{6}\cdot(2(\theta-\alpha)-\frac{\pi}{3})+2\Delta V_{1_{pu}}\right)d\theta\right]$$

or

$$U_{pu}=\frac{\cos\alpha+\cos(\alpha+\mu)}{2}+\left(\frac{3\mu^2}{4\pi}-\mu\right)\cdot\frac{\pi k^2}{6}\cdot I_{pu}+\left(2-\frac{3}{2\pi}\mu\right)\cdot\Delta V_{1_{pu}} \quad (17)$$

In order to facilitate physical interpretations, it is convenient to rewrite (17) using (6) expressed in p.u. values, resulting in

$$U_{pu}=\frac{\cos\alpha+\cos(\alpha+\mu)}{2}+\left(\frac{3\mu}{4\pi}-1\right)\cdot(\Delta V_{2_{pu}}-\Delta V_{1_{pu}}). \quad (18)$$

The first term in the equation above is identical to the expression for the DC-voltage in a conventional inductive commutated rectifier. Two contributions from the series capacitance have impact on the DC-voltage. The most significant is presented in the first term, meaning that capacitance lowers the overlap angle μ and thereby increases the DC-voltage. The contribution in the second term is negligibly small and is caused by a difference between the charging voltages of the incoming capacitor ΔV_{2pu}, and the outgoing capacitor ΔV_{1pu} during the overlap interval.

D. Valve voltage stress.

The peak voltages for capacitive commutation can substantially exceed those of inductive commutation, particularly for high k values (low capacitances). The valve voltage waveform in one cycle is separated into eight intervals; one is a straight line (valve conducts) and other seven are arc lines (see Figs 11 and 15). The peak voltage in each interval usually occurs at their boundaries and the valve peak voltage is the maximum among the intervals peak value.

V. CCC OPERATION ANALYSIS

Depending on k values, the AC branch impedance can be inductive (k<1) or capacitive (k>1). This paper considers only converter steady-state operation as rectifier with balanced capacitor voltages and within the normal load range where the commutations in both half-bridges circuits proceed independently.

A. Capacitive operation (k>1).

Figure 8 shows the behavior of the commutation angle μ as a function of DC current I_{pu} and firing angle α for different k values. The higher k (the smaller the capacitance) the more commutation-aiding voltage is produced for a particular DC current and the smaller is the overlap period. As a consequence, the maximum commutation angle never reaches 60°.

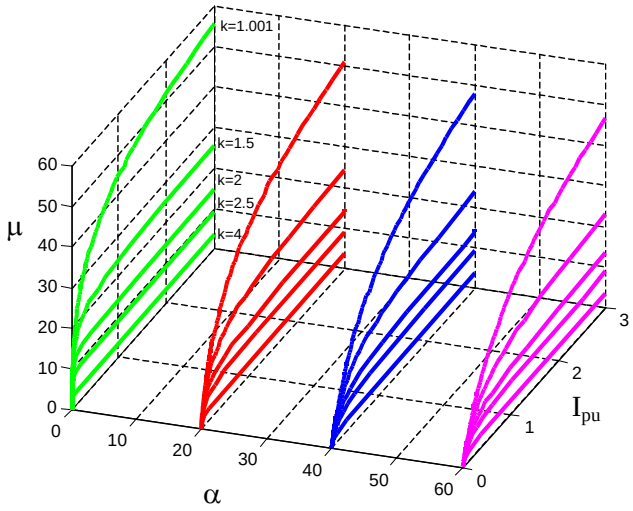

Fig. 8. Capacitive operation (k>1) - Curve relating overlap (μ) and firing (α) angles to DC current (I_{pu}) for different k values.

Figure 9 shows the DC voltage U_{pu} versus DC current I_{pu} characteristics for different firing angles α and k values. Comparing the DC characteristic for this case and for inductive commutation, it can be noticed that the capacitance diminishes the overlap angle μ improving DC voltage regulation characteristic for the same current conditions.

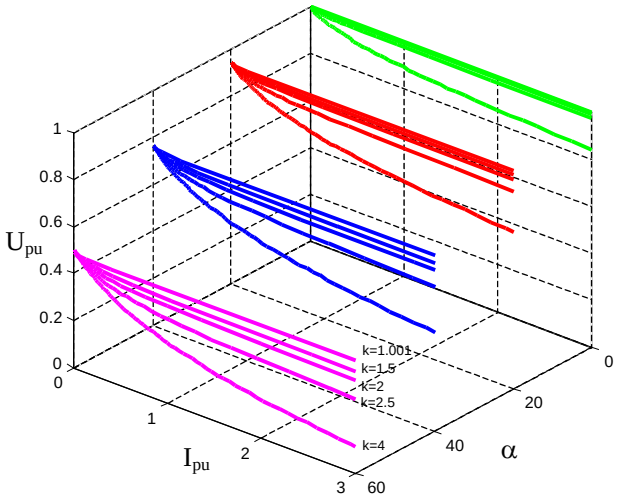

Fig. 9. Capacitive operation (k>1) - DC voltage (U_{pu}) versus DC current (I_{pu}) for different firing angles (α) and k values.

Figure 10 obtained from (15), with overlap angle limited to 0°≤μ≤60°, shows the extent to which the firing angle can

be advanced beyond the normal region (inductive commutation) as a function of DC current for different k values. Notice that in Figs. 10 and 13 the admissible operation region lies above the curves. Commutation cannot occur in the region below the curves. If the load current exceeds a minimum value, commutations can take place at any firing angle ($0<\alpha<360°$) whereby reactive power can be consumed or supplied by the converter.

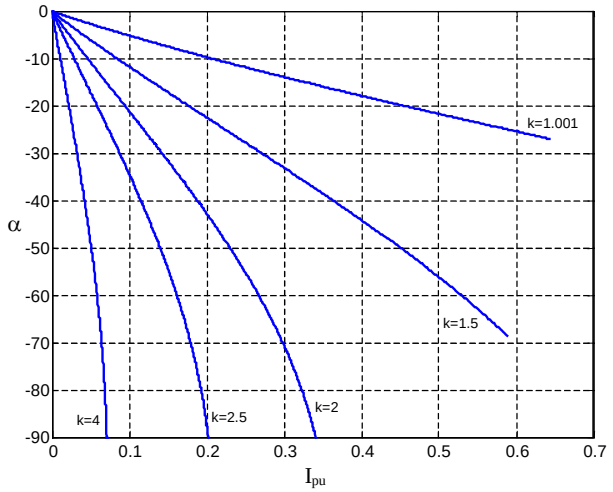

Fig. 10. Capacitive operation (k>1) – Admissible negative firing angle (α) versus DC current (I_{pu}) for different and k values.

Figure 11 shows the valve voltage waveform obtained by computational simulation for a given firing angle and dc current value and different k values and k=0 (inductive commutation).

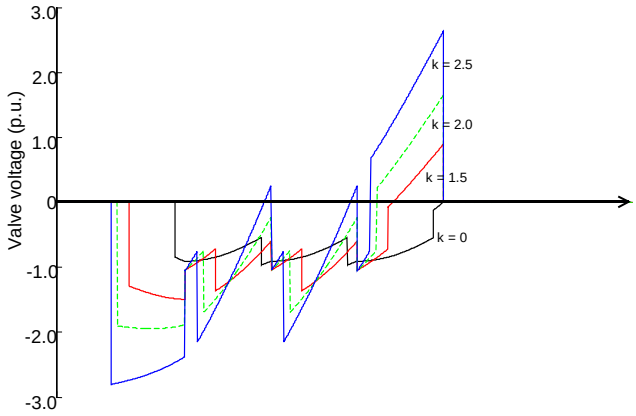

Fig. 11. Capacitive operation (k>1) – Valve voltage waveform for $\alpha=0°$, I_{pu} =0.5 and different and k values.

Notice that peak voltages of the valves can substantially exceed those for inductive commutation, particularly if capacitor values are small in order to achieve higher maximum firing angles. For a given capacitor value, the peak voltages are not necessarily exceeded, provided operation is restricted to certain range of firing angles and DC current. In a typical specification for HVDC systems, the valve stress is limited to approximately 110% of that of the conventional converter [8].

B. Inductive operation (k<1).

For k<1, an increase in capacitance tends to an effective short-circuit and operation tends to conventional inductive commutation for k=0.

Figure 12 shows the behavior of the commutation angle μ as a function of DC current I_{pu} and firing angle α for different k values. It can be noticed that for a particular current, the overlap angle is inversely proportional to k. Also, the current range where commutations in both half bridges occur independently (operation MODE 1 in Fig. 2) becomes larger.

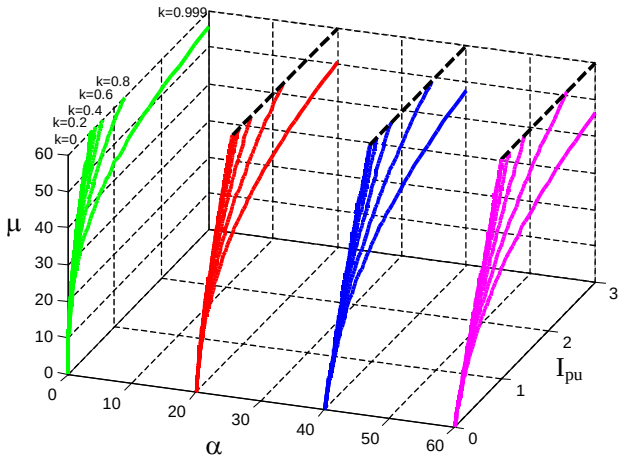

Fig. 12. Inductive operation (k<1) - Curve relating overlap (μ) and firing (α) angles to DC current (I_{pu}) for different k values.

Figure 13 shows the DC voltage U_{pu} versus DC current I_{pu} characteristics for different firing angles α and k values. Notice again that the presence of the capacitance C diminishes the overlap angle μ, improving DC voltage regulation for the same current conditions.

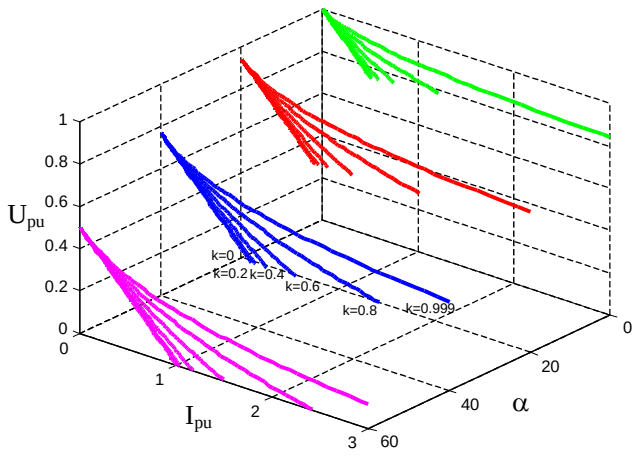

Fig. 13. Inductive operation (k<1) - DC voltage (U_{pu}) versus DC current (I_{pu}) for different firing angles (α) and k values.

Figure 14 was obtained from (15), with overlap angle limited to $0°\leq\mu\leq60°$. The region above the curve for a given k defines the range of negative firing angles as a function of DC current for which steady state operation is attainable. The smaller the capacitance (higher k), the more commutation-aiding voltage is produced for any given direct current.

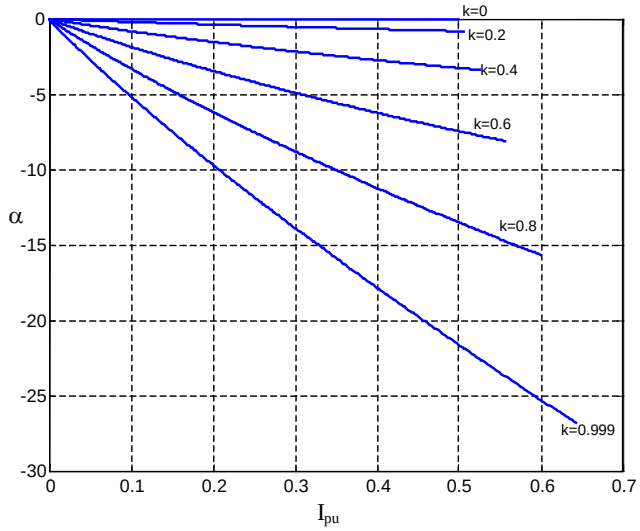

Fig. 14. Inductive operation (k<1) – Admissible negative firing angle (α) versus DC current (I_{pu}) for different and k values.

Figure 15 shows the valve voltage waveform obtained by computational simulation for a given firing angle and DC current value and different k values, including k=0 (inductive commutation).

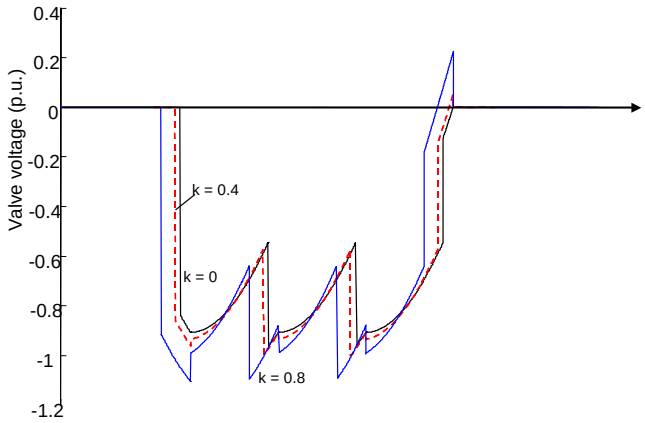

Fig. 15. Inductive operation (k<1) – Valve voltage waveform for α=0°, I_{pu} =0.5 and different and k values.

For k<1 the voltage stress on the valve is considerably lower than at capacitive operation, but the capacitance values are much higher.

VI. FINAL REMARKS

This paper presents a detailed mathematical analysis of the fundamental behavior in steady state operation of the bridge rectifier with series capacitances in the AC branches.

This converter operates with smaller overlap angles than the standard inductive commutated rectifiers, improving DC voltage regulation.

The capacitor values and DC current determine the admissible firing angle range. The operating range can be extended in the first and fourth quadrants by reducing capacitor value at the expense of higher valve voltage stress.

The desired operation range must be weighted against the necessary capacitor rating and any increased voltage stress imposed on the valves. During transient operation conditions, sudden changes in the firing angle can cause an appreciable increase in the valve conduction interval. Therefore, additional voltage limiting arresters are a required feature in the capacitors to protect them against overcharging.

The CCC is an attractive option for HVDC systems, where besides energy transmission, the converter has to deliver reactive power.

REFERENCES

[1] J. Reeve, J. A. Baron, G. A. Hanley, “Technical Assessment of Artificial Commutation of HVDC Converters with Series Capacitors”, IEEE Transactions on Power Apparatus and Systems, v. 87, n. 10, pp 1830-1840, 1968.

[2] G. Möltgen, “Line Commutated Thyristor Converters”, Siemens AG, 1972.

[3] W. Hartel, Stromrichterchaltungen, Berlin, Springer Verlag, 1977.

[4] S. Gomes Jr., T. Jonsson, D. Menzies, R. Ljungqvist, “Modeling Capacitor Commutated Converters in Power System Stability Studies”, IEEE Trans. on Power Systems, Vol. 17, No. 2, pp. 371-377, May 2002.

[5] M. Meisingset, “Application of capacitor commutated converters in multi-infeed HVDC-schemes”, Siemens Winnipeg, Manitoba, Canada, 2000.

[6] V. K. Sood, “HVDC and FACTS controllers”, Kluwer Academic Publishers, Massachusetts, USA 1st Edition, 2004.

[7] Y. Kazachkov, “Fundamentals of a Series Capacitor Commutated HVDC Terminal”, IEEE Transactions on Power Delivery, v. 13, n. 4, pp. 1157-1161, October 1998.

[8] W. Hammer, “Dynamic Modeling of Line and Capacitor Commutated Converters for HVDC Power Transmission”, Diss. Swiss. Fed. Inst. of Tech. Zurich.